Materials Advances

ROYAL SOCIETY OF CHEMISTRY

COMMUNICATION

View Article Online
View Journal | View Issue

Cite this: *Mater. Adv.*, 2026, 7, 187

Received 15th October 2025,
Accepted 27th November 2025

DOI: 10.1039/d5ma01190f

rsc.li/materials-advances

Sulfur-rich polymer with nanoparticles: high refractive index dual-tone photoresist

Xiaofei Qian *[ab] and Tao Liu[a]

A sulfur-containing polymer was synthesized and the refractive index (RI) reached 1.80 (633 nm) upon incorporation with nano TiO_2 particles. Mixtures were formulated as high RI dual-tone photoresists with high transparency by introducing a photoacid generator and crosslinker. The good patterning performance suggests potential applications in optical devices.

1. Introduction

High refractive index (RI) materials have attracted significant attention due to their diverse applications in lenses, augmented/virtual reality holographic technologies, optical devices, *etc.*[1,2] Inorganic materials usually exhibit high refractive indices ($n > 2.0$),[3] while their low flexibility and high density limit their applications.[4] Organic polymers could overcome the disadvantages and offer low weight, easy processability, and improved capability for fine-tuning properties through chemical modification.[5] However, traditional optical polymeric materials like PMMA or PS generally possess much lower refractive indices ($n \sim 1.3$–1.6).[6] Several methods have been employed to enhance the RI according to the Lorentz–Lorenz equation, and an effective method is to mix nanoparticles into the polymer matrix, such as TiO_2, ZrO_2, and ZnO, which have been well studied previously.[7–11] Another approach is to introduce aromatic groups, highly polarizable atoms like halogen atoms, sulfur, phosphorus or selenium.[12–14] Of these, sulfur-containing polymers with high RI have been extensively studied owing to the high atomic polarizability, good stability and abundant reserves.[15,16] Employing a monomer with S atoms in the polymerization process is a conventional way to obtain sulfur-containing polymers, such as sulfur-containing poly(methyl)acrylate,[17] polyimide,[18] polyphenylene sulfide,[19,20] and polysulfone,[21] which have been reported in a previous review.[22] The main drawback of this synthetic strategy is that the sulfur content depends on the monomer, limiting further increase of the RI. Elemental sulfur is an ideal sulfur source and is typically used in the synthesis of vulcanized rubber.[16] In 2013, Pyun and Char reported a new reaction protocol,[23] which reversed the established vulcanization process. In this polymerization procedure, molten sulfur served as both solvent and reagent. The S_8 ring opened at 185 °C and released free radicals to initiate polymerization with 1,3-diisopropenylbenzene (DIB). The content of sulfur could reach over 50% upon adjusting the feed ratio of the sulfur and monomer, and the polymer exhibited a high RI of about 1.8. When increasing the sulfur content, the RI of the polymers could reach 1.86 at 633 nm.[24] Further study of this reaction involved the introduction of selenium,[25] the use of organometallic monomers,[26] mechanochemical synthetic methodology,[27] *etc.* Though the inverse vulcanization process is suitable for a wide range of monomers,[28–31] the synthetic approach still faces challenges. The temperature of polymerization for inverse vulcanization was 185 °C, as previously reported.[23] Meanwhile, the process released toxic H_2S, which affected large-scale production. Wu and colleagues applied significant effort to improve the reaction process, and they introduced Zn diethyldithiocarbamate (DTC) salt to the reaction system to reduce the initiation temperature to 100–135 °C,[32,33] further utilizing UV light to assist the polymerization,[34] allowing the reaction to occur at room temperature. This synthetic protocol expanded the variety of sulfur-containing polymers and thereby broadened the potential applications,[35] such as in nanoimprinting,[36] lithium batteries,[37] long-wave infrared transparent polymers,[38,39] self-healing materials,[39,40] and metal ion capture resins.[41] The major problem with the inverse vulcanization product is that the polymer exhibits a dark red or brown colour, making it unsuitable for applications requiring high transparency. Thus, Im and coworkers reported a new method, sulfur chemical vapor deposition (sCVD),[42,43] in which elemental sulfur was evaporated by the apparatus and polymerized with the vapor-phase monomer. The transmittance remained over 90% in the visible region and the RI reached 1.98.[2] The synthetic method required complex apparatus and the heavily crosslinked polymer

[a] *School of Microelectronics, Fudan University, Shanghai, 200433, P. R. China. E-mail: xfqian@fudan.edu.cn*
[b] *Fudan Zhangjiang Institute, Shanghai, 201203, P. R. China*

film is deposited on the surface of the substrate, which complicated the patterning process. Inspired by KrF resin structures,[44] we synthesized a sulfur-rich photosensitive polymer, and upon incorporation with nano TiO_2, the spin-coated film exhibited a high RI of up to 1.80 (633 nm) with high transparency (film thickness 300 nm). We further explored the lithographic properties of the polymer under UV exposure to fabricate microstructures, and both positive and negative tone photoresists demonstrated promising photographic capabilities.

2. Results and discussion

A series of S-containing poly(methyl) acrylates was synthesized by using sodium thiophenolate as an activator. We started the exploration of the reaction using a feed ratio of [phenyl methacrylate]:[sulfur] = 2:1, and the homopolymer exhibited a high RI of 1.57.[45] As shown in Table 1, polar solvents such as DMF, NMP, and DMAc may assist in the cleavage of the S–S bond, which was mentioned in the previous literature.[46] It was found that the reaction worked well in DMF and DMAc, and the sulfur conversion reached 60% and 79%, respectively, after stirring for 24 h. The S content decreased a little from 38.5% to 37.6%, and the Mn of the polymers was increased from 2.1 kg mol^{-1} to 2.7 kg mol^{-1}. Surprisingly, when we used NMP as the reaction solvent, the sulfur was consumed within 6 hours. The elemental analysis shows that polymers synthesized in NMP contained 43.6% S and the M_n of 3.1 kg mol^{-1}. Increasing the monomer feed ratio to 5:1 reduced the S content to 32.7%., while further increasing it to 10:1 still maintained the S content above 30%, indicating a decreasing trend with increasing monomer feed ratio. Correspondingly, the M_n increased to 4.1 and 4.3 kg mol^{-1} at feed ratios of 5:1 and 10:1, respectively.

With the optimal reaction conditions, we extended the reaction to several methacrylates. As shown in Table 2, most methacrylates were suitable for the polymerization, including 2-naphthylmethyl acrylate (2-NMA), benzyl methacrylate (BzMA), 4-((tetrahydro-2*H*-pyran-2-yl)oxy)phenyl methacrylate (THPOPMA), adamantan-1-ylmethyl methacrylate (AdaMMA), methyl methacrylate (MMA), and butane-1,3-diyl bis(2-methylacrylate) (BDBMA).

Proton nuclear magnetic resonance (^{1}H NMR) was used to confirm the sulfide block of each polymer structure, and the spectrum (Fig. 1a) shows that the double bonds of PMA at 6.37 and 5.77 disappeared, while a broad peak was observed between 3.44 and 4.06, which can be attributed to the hydrogen signal of the polysulfide blocks. The peaks attributed to the protons of the methyl and aromatic groups became broadened. This confirmed that the monomer was polymerized, and the sulfur was inserted into the main chain. The Raman spectrum (Fig. 1b) was used to confirm the detailed structures. The C-S vibration peak[47] of the polymer matrix was observed at 717 cm^{-1}, and at low sulfur loadings of P(PMA$_{100}$-S$_{20}$) and P(PMA$_{200}$-S$_{20}$), a sharp signal at around 532 cm^{-1} corresponding to disulfide links was observed,

Table 1 Screening of the reaction conditions for the polymerization of phenyl methacrylate (PMA) with sulfur[a]

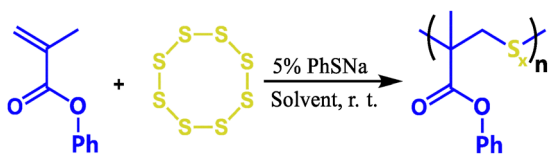

Entry	Feed ratio[b]	Solvent	Time (h)	Conv.[c]	S[d] (%)	M_n[e] (kg mol^{-1})
1	2:1	DMF	24	60	38.5	2.1
2	2:1	DMAc	24	79	37.6	2.7
3	2:1	NMP	6	>99	43.6	3.1
4	5:1	NMP	6	>99	32.7	4.1
5	10:1	NMP	6	>99	30.7	4.3

[a] Unless otherwise specified, the reaction conditions were: S_8 0.256 g (1 mmol); monomer and PhSNa feed ratio as specified; 2 mL of solvent; under argon. [b] Feed ratio: [monomer]:[S_8]. [c] Conversion was calculated from unreacted sulfur. [d] S content % was determined by elemental analysis. [e] M_n was determined by GPC.

Table 2 Scope of methyl acrylates in the reaction with sulfur[a]

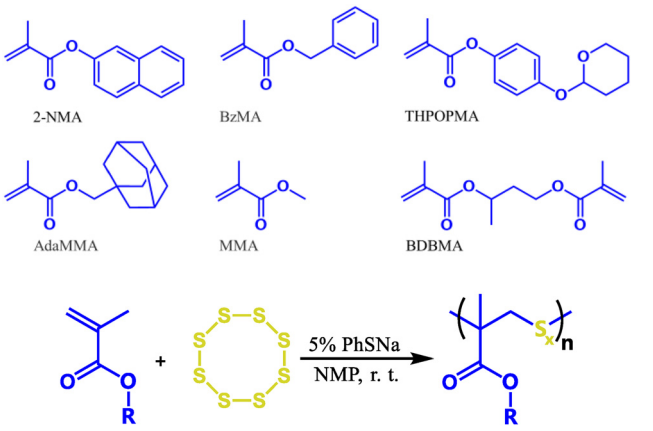

Entry	Monomer	Conv.[b]	S[c] (%)	M_n[d] (kg mol^{-1})
1	2-NMA	70	33.9	2.5
2	MMA	>99	48.5	2.2
3	AdaMMA	88	25.8	1.6
4	BzMA	>99	39.6	2.3
5	THPOPMA	>99	28.8	3.9
6	BDBMA	>99	38.1	—

[a] Unless otherwise specified, the reaction conditions were: S_8 0.256 g (1 mmol); monomer 2 mmol; PhSNa 0.05 mmol; 2 mL of NMP; under argon. [b] Conversion was calculated from unreacted sulfur. [c] S content % was determined by elemental analysis. [d] M_n was determined by GPC.

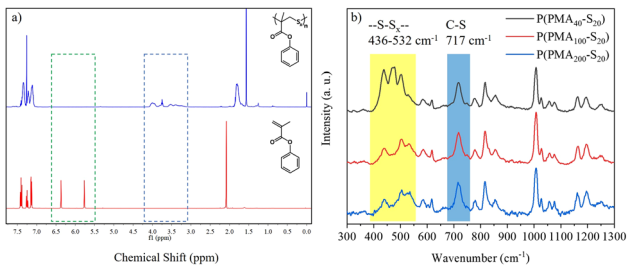

Fig. 1 (a) ^{1}H NMR spectra of P(PMA$_{40}$-S$_{20}$) and the PMA monomer. (b) Raman spectra of polymers with different feed ratios.

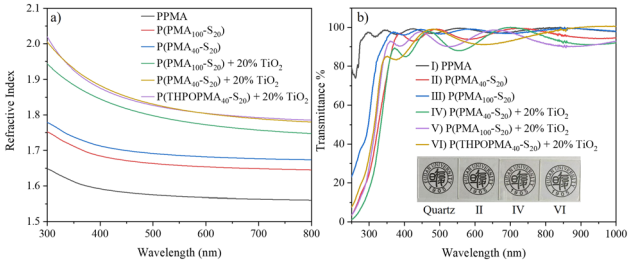

Fig. 2 (a) Refractive indices of the polymers (film thickness ~300 nm). (b) Transmittance spectra of the polymers (film thickness ~300 nm).

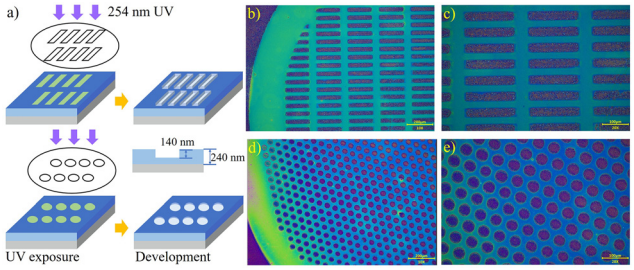

Fig. 3 (a) General lithography process for a positive tone photoresist with a rectangle and hole pattern. (b) and (c) After development inspection (ADI) image under an optical microscope (205 × 37 μm rectangle pattern). (d) and (e) ADI image under an optical microscope (75 μm hole pattern).

while at high sulfur loadings of P(PMA_{40}-S_{20}), trisulfide (-S-S-S-) and tetrasulfide (-S-S-S-S-) were predominant at 436–500 cm^{-1}.[48]

Differential scanning calorimetry (DSC) curves were recorded to confirm the sulfur residue in the polymers (Fig. S3). Characteristic peaks of S were observed at 109 °C and 123 °C, while no signals were found at that temperature for the designed polymers, which could confirm the consumption of sulfur. The T_g of P(PMA_{40}-S_{20}) was measured as 1.7 °C, and with decreasing sulfur content, the T_g was increased to 19.9 °C and 21.3 °C. The T_g of the polymers exhibited a downward trend as the S content was increased.

The optical properties are vital for application in AR/VR devices. As shown in Fig. 2a, the RI of the homopolymer PPMA is 1.57 at 633 nm, which is consistent with the literature,[45] and the Abbe number was calculated to be 51.6 (Table S3). As the sulfur was inserted into the main chain of P(PMA_{100}-S_{20}) with 32.7% S content, the RI increased to 1.65 at 633 nm, and the Abbe number decreased to 43.7. When the sulfur content reached 43.6%, the RI increased to 1.68 correspondingly and the Abbe number remained at 42.7. To further enhance the RI, we mixed nano TiO_2 with the polymers. 20% weight of TiO_2 was blended with P(PMA_{100}-S_{20}) and P(PMA_{40}-S_{20}), and the RI of the nanocomposite increased to 1.76 and 1.80, respectively, while the Abbe number decreased to 19.9 and 20.1. The transparency of the polymer film was measured using a UV-Vis spectrophotometer at a film thickness of about 300 nm. The homopolymer of PMA maintained over 90% transmittance in the visible region, while the transmittance remained over 90% at 400–1000 nm for P(PMA_{40}-S_{20}) and P(PMA_{100}-S_{20}), but decreased quickly in the 250–400 nm range. After blending with nano TiO_2 particles, the transparency decreased to 80–90% in the 400–1000 nm region, and it rapidly decreased at 250–400 nm with a cutoff wavelength of 250 nm. To demonstrate the optical properties of the material, we applied a thin film approximately 300 nm in thickness onto a quartz substrate and covered it with a logo, and it could be observed that all the films exhibited good transparency.

The application of high RI polymers in AR/VR displays needs high precision nanostructures, and lithography is one of the most feasible and mature methods to fabricate nanostructures in industry, enabling large-scale production. Fig. 3a shows a typical procedure for lithography. A photoresist is spin coated on a wafer and exposed to UV light through a designed mask. We designed the monomer of THPOPMA with dihydropyran as a protecting group, which was suitable for a photoresist. Through the polymerization method, the P($THPOPMA_{40}$-S_{20}) was synthesized, and the polymer with 20% TiO_2 exhibited a RI of 1.80 and transparency of over 80% in the visible region (Fig. 2a and b). The P($THPOPMA_{40}$-S_{20}) was blended with 3% weight photo acid generator (PAG) of triphenylsulfonium 1,1,2,2,3,3,4,4,4-nonafluorobutane-1-sulfonate (TPS) and 20% weight of nano TiO_2 particles to form a photoresist. The mixture was dissolved in propylene glycol methyl ether acetate (PGMEA, 8% solid content) as a high RI positive tone photoresist and spin coated on the Si substrate, covering both a rectangle and hole pattern Cu mask (205 × 37 μm rectangle and 75 μm hole pattern), and the exposure process was carried out under a 254 nm lamp for 1 min. After developing in standard 2.38% tetramethylammonium hydroxide (TMAH), the rectangle structure (Fig. 3b and c) and hole structure (Fig. 3d and e) were successfully transferred to the high RI surface with a step height of 140 nm.

Low molecular weight linear polymers are usually not resistant to solvents. To enhance the mechanical properties and resistance of the pattern structures, a study of a crosslinked negative tone high RI photoresist was conducted. Another 30% weight of trimethylolpropane triglycidyl ether was added to the previous solution as a crosslinker. The exposure time was extended to 30 min to ensure complete cross-linking, as shown in Fig. 4a. After developing in *n*-butyl acetate for 1 min, the negative patterns of the rectangle (Fig. 4b and c) and hole (Fig. 4d and e) were transferred to the surface with a step height of 60 nm.

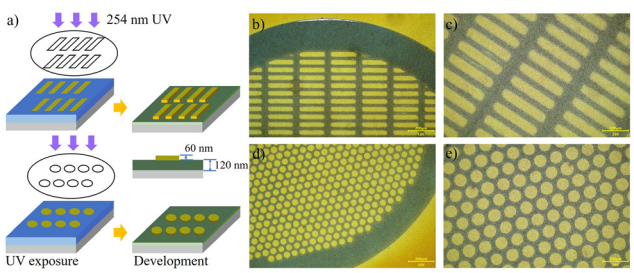

Fig. 4 (a) General lithography process for a negative tone photoresist with a rectangle and hole pattern. (b) and (c) ADI image under an optical microscope (205 × 37 μm rectangle pattern). (d) and (e) ADI image under an optical microscope (75 μm hole pattern).

3. Conclusions

In this study, the introduction of nano TiO_2 particles into a sulfur-rich polymer increased the RI from 1.68 to 1.80 (633 nm), and the transmittance remained over 80% in the visible region (film thickness 300 nm). Furthermore, the mixture formulated with a PAG and crosslinker consists of a dual-tone photoresist. Both positive tone and negative tone patterning capabilities were explored, demonstrating good lithographic performance and potential application in optical devices.

Author contributions

The manuscript was written through contributions of all authors. All authors have given approval to the final version of the manuscript.

Conflicts of interest

There are no conflicts to declare.

Data availability

The data supporting this article have been included as part of the supporting information (SI). Supporting information: monomer preparation, polymerization and lithography procedure, ^{1}H NMR spectra, DSC curves, and GPC curves. Supplementary information is available. See DOI: https://doi.org/10.1039/d5ma01190f.

Acknowledgements

This work was sponsored by the Natural Science Foundation of Shanghai No. 23ZR1425100.

Notes and references

1 Y. T. Zhou, Z. C. Zhu, K. Zhang and B. Yang, *Macromol. Rapid Commun.*, 2023, **44**, 2300411.
2 W. Jang, K. Choi, J. S. Choi, D. H. Kim, K. Char, J. Lim and S. G. Im, *ACS Appl. Mater. Interfaces*, 2021, **13**, 61629.
3 J. Loste, J. M. Lopez-Cuesta, L. Billon, H. Garay and M. Save, *Prog. Polym. Sci.*, 2019, **89**, 133.
4 Y. Wuliu, W. Dong, G. Huang, H. Xie, P. Yao, J. Tan, K. Mu, Z. Zhang, Y. Chen, M. Wang, L. Tian, C. Zhu and J. Xu, *Angew. Chem., Int. Ed.*, 2025, **64**, e202419446.
5 D. H. Kim, W. Jang, K. Choi, J. S. Choi, J. Pyun, J. Lim, K. Char and S. G. Im, *Sci. Adv.*, 2020, **6**, eabb5320.
6 J. Pyun and R. A. Norwood, *Prog. Polym. Sci.*, 2024, **156**, 101865.
7 W. Zhang, J. Min, H. Wang, H. Wang, X. L. Li, S. T. Ha, B. Zhang, C. F. Pan, H. Li, H. Liu, H. Yin, X. Yang, S. Liu, X. Xu, C. He, H. Y. Yang and J. K. W. Yang, *Nat. Nanotechnol.*, 2024, **19**, 1813.
8 K. Enomoto, M. Kikuchi, A. Narumi and S. Kawaguchi, *ACS Appl. Mater. Interfaces*, 2018, **10**, 13985.
9 C. Lü and B. Yang, *J. Mater. Chem.*, 2009, **19**, 2884.
10 C. H. Park, J. G. Kim, S. G. Jung, D. J. Lee, Y. W. Park and B. K. Ju, *Sci. Rep.*, 2019, **9**, 8690.
11 C. L. Tsai and G. S. Liou, *Chem. Commun.*, 2015, **51**, 13523.
12 Y. Wuliu, G. Huang, J. Tan, W. Dong, H. Huang, K. Mu, L. Feng, M. Wang, L. Tian, C. Zhu and J. Xu, *Macromolecules*, 2023, **56**, 9881.
13 C. Pitois, D. Wiesmann, M. Lindgren and A. Hult, *Adv. Mater.*, 2001, **13**, 1483.
14 K. Mazumder, B. Voit and S. Banerjee, *ACS Omega*, 2024, **9**, 6253.
15 D. A. Boyd, *Angew. Chem., Int. Ed.*, 2016, **55**, 15486.
16 T. J. Yue, W. M. Ren and X. B. Lu, *Chem. Rev.*, 2023, **123**, 14038.
17 R. Okutsu, S. Ando and M. Ueda, *Chem. Mater.*, 2008, **20**, 4017.
18 N. H. You, Y. Suzuki, D. Yorifuji, S. Ando and M. Ueda, *Macromolecules*, 2008, **41**, 6361.
19 S. Watanabe and K. Oyaizu, *Macromolecules*, 2022, **55**, 2252.
20 K. Nakabayashi, T. Imai, M. C. Fu, S. Ando, T. Higashihara and M. Ueda, *J. Mater. Chem. C*, 2015, **3**, 7081.
21 R. Okutsu, Y. Suzuki, S. Ando and M. Ueda, *Macromolecules*, 2008, **41**, 6165.
22 T. Higashihara and M. Ueda, *Macromolecules*, 2015, **48**, 1915.
23 W. J. Chung, J. J. Griebel, E. T. Kim, H. Yoon, A. G. Simmonds, H. J. Ji, P. T. Dirlam, R. S. Glass, J. J. Wie, N. A. Nguyen, B. W. Guralnick, J. Park, A. Somogyi, P. Theato, M. E. Mackay, Y. E. Sung, K. Char and J. Pyun, *Nat. Chem.*, 2013, **5**, 518.
24 J. J. Griebel, S. Namnabat, E. T. Kim, R. Himmelhuber, D. H. Moronta, W. J. Chung, A. G. Simmonds, K. J. Kim, J. van der Laan, N. A. Nguyen, E. L. Dereniak, M. E. Mackay, K. Char, R. S. Glass, R. A. Norwood and J. Pyun, *Adv. Mater.*, 2014, **26**, 3014.
25 L. E. Anderson, T. S. Kleine, Y. Zhang, D. D. Phan, S. Namnabat, E. A. LaVilla, K. M. Konopka, L. R. Diaz, M. S. Manchester, J. Schwiegerling, R. S. Glass, M. E. Mackay, K. Char, R. A. Norwood and J. Pyun, *ACS Macro Lett.*, 2017, **6**, 500.
26 D. A. Boyd, V. Q. Nguyen, C. C. McClain, F. H. Kung, C. C. Baker, J. D. Myers, M. P. Hunt, W. Kim and J. S. Sanghera, *ACS Macro Lett.*, 2019, **8**, 113.
27 P. Y. Yan, W. Zhao, F. McBride, D. Cai, J. Dale, V. Hanna and T. Hasell, *Nat. Commun.*, 2022, **13**, 4824.
28 J. Bao, K. P. Martin, E. Cho, K. S. Kang, R. S. Glass, V. Coropceanu, J. L. Bredas, W. O. Parker Jr., J. T. Njardarson and J. Pyun, *J. Am. Chem. Soc.*, 2023, **145**, 12386.
29 J. M. Scheiger, M. Hoffmann, P. Falkenstein, Z. Wang, M. Rutschmann, V. W. Scheiger, A. Grimm, K. Urbschat, T. Sengpiel, J. Matysik, M. Wilhelm, P. A. Levkin and P. Theato, *Angew. Chem., Int. Ed.*, 2022, **61**, e202114896.
30 B. Zhang, S. Petcher and T. Hasell, *Chem. Commun.*, 2019, **55**, 10681.
31 J. A. Smith, S. J. Green, S. Petcher, D. J. Parker, B. Zhang, M. J. H. Worthington, X. F. Wu, C. A. Kelly, T. Baker, C. T. Gibson, J. A. Campbell, D. A. Lewis, M. J. Jenkins, H. Willcock, J. M. Chalker and T. Hasell, *Chem. – Eur. J.*, 2019, **25**, 10433.

32 X. F. Wu, J. A. Smith, S. Petcher, B. Zhang, D. J. Parker, J. M. Griffin and T. Hasell, *Nat. Commun.*, 2019, **10**, 647.
33 L. J. Dodd, Ö. Omar, X. F. Wu and T. Hasell, *ACS Catal.*, 2021, **11**, 4441.
34 J. Jia, J. Liu, Z. Q. Wang, T. Liu, P. Yan, X. Q. Gong, C. Zhao, L. Chen, C. Miao, W. Zhao, D. Cai, X. C. Wang, A. I. Cooper, X. F. Wu, T. Hasell and Z. J. Quan, *Nat. Chem.*, 2022, **14**, 1249.
35 Y. Zhang, R. S. Glass, K. Char and J. Pyun, *Polym. Chem.*, 2019, **10**, 4078.
36 C. P. Ambulo, K. J. Carothers, A. T. Hollis, H. N. Limburg, L. Sun, C. J. Thrasher, M. E. McConney and N. P. Godman, *Macromol. Rapid Commun.*, 2023, **44**, 2200798.
37 M. Arslan, B. Kiskan, E. C. Cengiz, R. Demir-Cakan and Y. Yagci, *Eur. Polym. J.*, 2016, **80**, 70.
38 M. Lee, Y. Oh, J. Yu, S. G. Jang, H. Yeo, J. J. Park and N. H. You, *Nat. Commun.*, 2023, **14**, 2866.
39 J. J. Griebel, N. A. Nguyen, S. Namnabat, L. E. Anderson, R. S. Glass, R. A. Norwood, M. E. Mackay, K. Char and J. Pyun, *ACS Macro Lett.*, 2015, **4**, 862.
40 Z. Yang, P. Yan, X. Li, C. Miao, D. Cai, W. Ji, M. Song, L. J. Dodd, X. F. Wu, T. Hasell and P. Song, *Polym. Chem.*, 2023, **14**, 3686.
41 D. Cai, J. J. Dale, S. Petcher, X. Wu and T. Hasell, *Chem. – Eur. J.*, 2024, **30**, e202402194.
42 K. Choi, W. Jang, W. Lee, J. S. Choi, M. Kang, J. Kim, K. Char, J. Lim and S. G. Im, *Macromolecules*, 2022, **55**, 7222.
43 W. Jang, K. Choi, M. Kang, S. Park, D. H. Kim, J. Ahn, H. Lim, K. Char, J. Lim and S. G. Im, *Chem. Mater.*, 2023, **35**, 8181.
44 D. P. Sanders, *Chem. Rev.*, 2010, **110**, 321.
45 J. W. Gooch, Appendix C: Polymer Properties, *Encyclopedic Dictionary of Polymers*, Springer, New York, NY, 2011, p. 860.
46 P. Y. Yan, W. Zhao, S. J. Tonkin, J. M. Chalker, T. L. Schiller and T. Hasell, *Chem. Mater.*, 2022, **34**, 1167.
47 J. Wręczycki, D. M. Bieliński, M. Kozanecki, P. Maczugowska and G. Mlostoń, *Materials*, 2020, **13**, 2597.
48 C. Gallizioli, D. Battke, H. Schlaad, P. Deglmann and A. J. Plajer, *Angew. Chem., Int. Ed.*, 2024, **63**, e202319810.